2002

Conceptual and scaling evaluation of vehicle traffic thermal effects on snow/ice-covered roads

Joseph M. Prusa
Iowa State University

Moti Segal
Iowa State University, segal@iastate.edu

Bradley R. Temeyer
Iowa State University

William A. Gallus Jr.
Iowa State University, wgallus@iastate.edu

Eugene S. Takle
Iowa State University, gstakle@iastate.edu

Conceptual and Scaling Evaluation of Vehicle Traffic Thermal Effects on Snow/Ice-Covered Roads*

JOSEPH M. PRUSA

Department of Mechanical Engineering, Iowa State University, Ames, Iowa

MOTI SEGAL

Agricultural Meteorology Program, Department of Agronomy, Iowa State University, Ames, Iowa

BRADLEY R. TEMEYER AND WILLIAM A. GALLUS JR.

Department of Geological and Atmospheric Sciences, Iowa State University, Ames, Iowa

EUGENE S. TAKLE

Agricultural Meteorology Program, Department of Agronomy, and Department of Geological and Atmospheric Sciences, Iowa State University, Ames, Iowa

(Manuscript received 23 November 2001, in final form 8 June 2002)

ABSTRACT

The potential thermal effects of traffic on road surface thermal energy balance under frost/snow cover conditions have been largely ignored in meteorological evaluations of road ice deposit conditions. Preliminary exploration of these effects, particularly for heavy traffic scenarios with calm wind conditions and an ambient temperature of 0°C, is provided in this study using a conceptual model. Observational data were used to constrain the model, and parameterizations were employed to estimate the various heat transfer processes involved. The results indicate that, for heavy traffic situations, as well as for stopped traffic at intersections, the traffic thermal flux contribution at the surface is noticeable in a wide range of possible frost/snow-covered road conditions. The sensitivity to variation in traffic density, speed, and the emissivity of vehicle radiative surfaces, among others, is evaluated. Simple quantification of these traffic thermal effects, which might be considered in operational meteorological model forecasting of icy road conditions, is offered.

1. Introduction

Accumulation of snow or ice on roads generates potentially hazardous traffic conditions. Considerable effort has been given to meteorological forecasting of this adverse transportation condition, particularly for road freezing conditions (e.g., Rayer 1987; Takle 1990; Bogren et al. 1992; Sass 1992; Brown and Murphy 1996). However, the incorporation of the thermal effect of the traffic itself on these icy road deposits in forecasting models of road conditions has been largely ignored or is incomplete. The goal of this paper is to provide a conceptual and scaling evaluation of traffic thermal flux contributions to the road surface by evaluating various vehicle heat sources generated by fuel consumption—an approach that is not reported in the literature. The present formulation for traffic thermal effects might be considered in operational model forecasting of icy road conditions. We provide illustrative quantification for the thermal flux generated by high traffic density when the background wind is calm.

Thermal vehicle effects that influence road ice deposits are

1) replacement of the atmospheric downwelling infrared radiation (IR) with IR emission from the bottom of the vehicle (of particular significance are IR emissions from the heated engine, transmission, and exhaust pipe system of the vehicle to the road surface),
2) turbulent convective heat exchange induced by vehicle motion from the warm surfaces of the vehicle to the road ice deposits,

* Journal Paper No. 19400 of the Iowa Agriculture and Home Economics Experiment Station.

Corresponding author address: Dr. Joseph M. Prusa, Teraflux Corporation, 952 NW 8th St., Boca Raton, FL 33486.
E-mail: prusa@iastate.edu

3) frictional heat dissipation through traction effect of the tires on the road,
4) sensible heat and moisture fluxes onto the road surface from hot exhaust gases (including water vapor emitted from the vehicle following fuel combustion), and
5) downward air heat flux caused by the turbulence generated by aerodynamic drag associated with the vehicle's movement.

The potential influence of each of these thermal effects on the surface heat balance of road ice deposits is evaluated for several basic traffic scenarios: freely moving vehicles in urban and highway settings, and vehicles stopped at an intersection.

To generate mechanical work to move a vehicle, fuel is oxidized in an internal combustion (IC) engine to produce energy. The efficiency of typical IC engines is in the range 15%–35% depending on the engine type, driving conditions, and speed (Heywood 1988). Higher efficiencies typically occur with continuous traffic movement (e.g., not stop-and-go traffic conditions) and higher speeds. The work done on the piston by the expanding gases provides the mechanical energy required for the movement of the vehicle. If there is no change in the elevation of the road, the mechanical energy ultimately dissipates completely into heat through the rolling friction resistance of tires, aerodynamic drag of the vehicle, and losses in the power train (e.g., transmission, axles) and other secondary sources (e.g., accessories, air conditioner).

We note that any change in the vehicle potential energy is insignificant except in the most mountainous cases: for a 1000-kg vehicle, an altitude change of 4.5 km is required to match the 45 MJ energy content (or, equivalently, enthalpy of combustion) of 1 kg of gasoline. Given the enthalpy of combustion of the fuel and its consumption rate, the total heat generation rate attributed to each of the above-listed thermal effects by a vehicle can be estimated.

Heat of combustion is also lost directly through processes 1, 2, and 4 mentioned above. The engine cooling system, using water, oil, and/or air as working fluids typically removes 30%–60% of the ideal heat of combustion. The bulk of this heat is efficiently transferred by convection into the ambient atmosphere in the immediate vicinity of the vehicle. The cooling system typically removes a greater fraction of heat at lower speeds. The ratio of coolant heat flux to mechanical power ranges from 3:1 to 2:1 for low to high vehicle speeds, respectively (Heywood 1988). Only a small amount of heat is directly radiated from the engine as an IR emission because the body of the vehicle acts as a radiation shield and blocks this loss process. Exhaust gases leave the engine at elevated temperatures and typically carry about 25%–35% of the ideal heat of combustion. The effect of traffic on the downward thermal flux can be inferred qualitatively and indirectly by comparing dry road surface temperatures as measured with dense and light traffic. However, observational studies on the thermal effects of dense traffic on dry road skin temperature are sparse. In an assessment of two motorways in Birmingham, Britain, Surgue et al. (1983) reported that recorded road surface temperatures were usually several degrees Celsius higher in the motorway where traffic was heaviest. Shao (1990) compared differences in surface temperatures at the same location between slow and fast traffic lanes for January–April of 1988. He found higher temperatures in the slow lane. This feature was most noticeable during morning and evening rush hours, especially in the afternoon when the temperature difference between the lanes was as high as 1°C. A few days of observations at Gothenburg, Sweden, by Gustavsson and Bogren (1991) suggest maximum corresponding differences of 1.5°C. Road skin temperature observations in Des Moines, Iowa, during the 1996/97 winter by Knollhoff (2001) suggest about 1.5°C traffic thermal contribution to the surface skin temperature, thus indicating a detectable thermal effect of traffic on road skin temperature.

The effect of heat released by vehicles on a characteristic unit area of road ice is related to the density of the traffic (i.e., percentage of the road area covered by vehicles) and to ambient temperatures. For simplicity of the evaluations, in this study an ambient temperature (i.e., the road temperature and the near-surface air temperature) of about 0°C is assumed. Thus, any net thermal flux gain from the traffic would contribute to ice melting. The traffic density is assumed to be high, though realistically so. As such, the model for the estimation of traffic thermal effects on snow/ice developed in the following sections will provide an upper limit for these effects. These results are based upon a characteristic midsize vehicle of known kilometerage (distance in kilometers traveled by consuming 1 L of fuel) in several different driving scenarios. Additional observations were made to compute the rolling friction coefficient (on dry pavement with good tires) and to measure the exhaust system exit plume temperature and characteristic outer engine temperature. The exhaust system exit temperatures provided an observational constraint on the exhaust system model sketched in appendix A. The drag coefficient was computed by following the method of Munson et al. (1990), given the known geometry of the vehicle.

Detailed results are presented in the following sections for four driving scenarios:

1) stopped urban traffic (UST),
2) moving urban traffic in heavy snow cover (UHS),
3) moving urban traffic in light snow cover/frost-covered road conditions (ULS), and
4) moving highway traffic in light snow cover/frost-covered road conditions (HLS).

In each of the light snow/frost-covered road conditions scenarios, the degree of snow/ice covering the road is

TABLE 1. Vehicle parameters for the various driving scenarios.

Parameter	Driving scenario			
	Urban stopped traffic (UST)	Urban heavy snow (UHS)	Urban light snow (ULS)	Highway light snow (HLS)
Vehicle spacing S (m)	3	25	15	50
Traffic speed V (m s^{-1})	0	10	15	30
Rolling friction coefficient μ	—	0.05	0.01	0.01
Kilometerage K (km L^{-1})	—	6.4	9.4	10.2
Traffic frequency f (s^{-1})	—	0.3	0.8	0.5
*Fuel consumption rate $\dot{m}_{\text{fuel}}$ (kg s^{-1})	0.0005	0.0011	0.0011	0.0020
Max road surface thermal flux $e_{\max}$ (kW m^{-2})	1.6	1.0	1.4	1.0

* The UST value is based upon polynomial extrapolation of non-UST values for the limit $V \to 0$.

assumed to be so small as to have negligible effect on vehicle traction. Thus the speed, spacing, and rolling friction coefficients are the same as for dry pavement. The traffic parameters characterizing these scenarios are presented in Table 1.

Sections 2–4 present a scaling evaluation and model results for the transport processes involved in the analysis. The effects of traffic on surface net thermal flux and thus the potential effect on ice melting or freeze suppression are summarized in section 5. Also included in section 5 is a sensitivity evaluation to variations in traffic/vehicle characteristics. Results obtained for the four different driving scenarios listed above are summarized in Tables 1–7. Although we have made an effort to quantify numerous effects that are important, our evaluations should be considered preliminary because some very basic model input parameters are subject to wide variations. Vehicle parameters such as kilometerage, engine efficiency, radiative surface characteristics, rolling friction coefficients, and vehicle drag coefficients, among others, are all subject to significant variations with vehicle type and condition, as well as driving style. Variations in environmental factors, such as ambient temperature, snow/ice density, wind, type of precipitation, and road surface (e.g., asphalt or concrete, presence of ice melting chemicals, condition of the surface) are also extremely important. To convey the magnitude of these variations/uncertainties, we use the two relational symbols $\sim$ and $\approx$. Symbol $\sim$ denotes approximately, about, within 30%–50% of a ''correct'' value, implication of that range of values, or functional dependency of a scale. Symbol $\approx$ denotes close to, within a few percent of a correct value, or implication of a small range of values.

2. Evaluations of thermal fluxes generated by vehicles

We begin by estimating the total amount of heat generated by a vehicle in traffic, thus providing an upper limit to potential thermal effects. Only a small amount of this heat affects the road surface. In the sections that follow, all uppercase variables pertaining to energy generation rates are extensive (e.g., E has dimension of power), whereas all associated lowercase variables are intensive (e.g., e has dimension of power divided by area, i.e., thermal flux). In this paper, we assume ideally that e is uniform in its area of definition.

a. The total heat generated by a vehicle

For all traffic scenarios, we consider the quasi-steady effect of a series of vehicles of width $W_v(\sim 1.7$ m) and length $L(\sim 5$ m) traveling in a given lane. These vehicles are assumed to travel at a uniform speed V and spacing S (see Fig. 1 for schematic illustration). An upper limit for the surface heat flux incident upon the road can be estimated by assuming that all the fuel energy ultimately reaches the road surface:

$$e_{\max} = \frac{E_{\text{tot}}}{W_v(L + S)}, \tag{1}$$

where E_{tot} is the total energy generation rate of the vehicle. Assuming perfect combustion, this generation rate

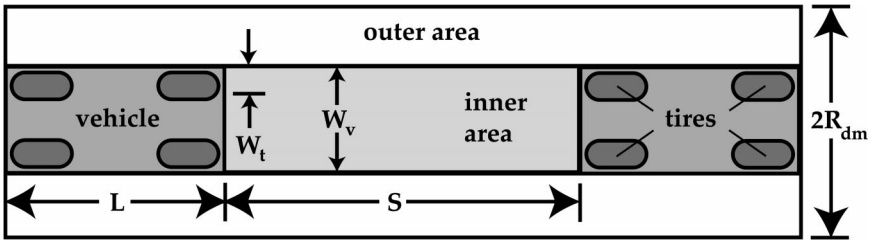

FIG. 1. Vehicle size and spacing parameters.

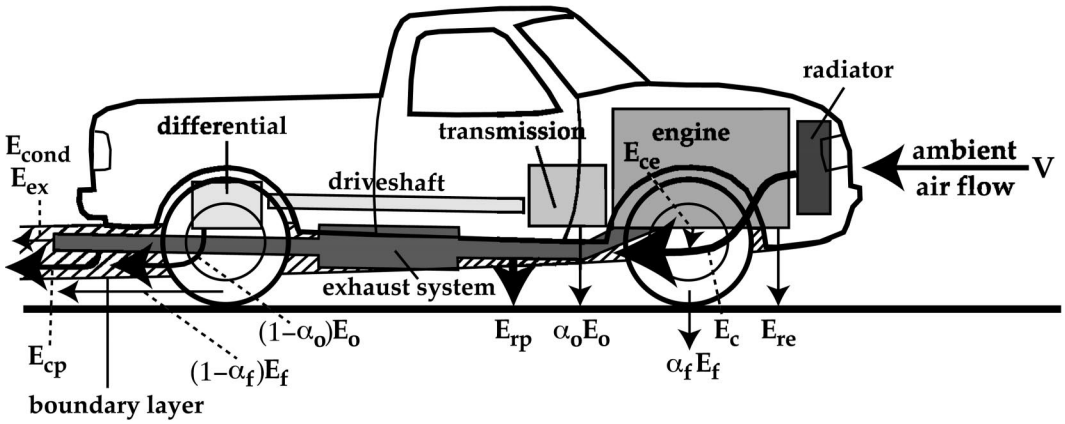

FIG. 2. Schematic illustration of the thermal energy flows from the vehicle to its surroundings. All radiated thermal flows are depicted by vertical arrows pointing straight down into the road. All convective thermal energy flows (with exception of thermal energy from the tires) leave the vehicle through the boundary layer. Once the boundary layer emerges from the rear of the vehicle, it rapidly loses its structure and its contents are mixed into the larger dissipative air mass. The sizes of the energy flow arrows approximate the magnitudes of the flows. Other losses E_o are represented here only by the major drivetrain components. The cooling system is depicted only by the radiator component.

requires a fuel mass flow rate of $\dot{m}_{\text{fuel}} = \rho_{\text{fuel}} V/K$, where ρ_{fuel} is the fuel density and K is the vehicle kilometerage, defined earlier.

For a moving vehicle, $E_{\text{tot}} = \lambda_{\text{fuel}} \dot{m}_{\text{fuel}}$, where λ_{fuel} is the enthalpy of combustion of the fuel. In our urban light snow scenario, we use $K \sim 9.4$ km L^{-1}, $V \sim 15$ m s^{-1}, and $S \sim 15$ m (three vehicle lengths). Given that $\rho_{\text{fuel}} = 0.67$ kg L^{-1} and $\lambda_{\text{fuel}} = 45$ MJ kg^{-1} for liquid octane (our approximation for gasoline), for the ULS scenario $\dot{m}_{\text{fuel}} = 1.1 \times 10^{-3}$ kg s^{-1} and $E_{\text{tot}} = 49$ kW. Using Eq. (1) yields $e_{\max} = 1.4$ kW m^{-2}. When the traffic is very slow or is stopped at intersections by traffic lights or stop signs—the UST scenario—Eq. (1) still applies but E_{tot} can no longer be determined directly from the fuel kilometerage, because $K \to 0$ when $V \to 0$. Based upon the known kilometerage at nonzero speeds (and hence fuel consumption rate), $\dot{m}_{\text{fuel}}$ for idling conditions during the UST scenario was extrapolated, yielding $E_{\text{tot}} = 22$ kW for this traffic scenario. A further assumption that the spacing between vehicles is reduced to $S \sim 3$ m yields a limiting surface flux of $e_{\max} = 1.6$ kW m^{-2} at intersections.

For moving traffic, computations may also be based upon traffic frequency f (number of vehicles crossing a given road section per second) rather than vehicle spacing S. These two variables are related according to $f = V/(L + S)$. For the ULS scenario, $f \approx 0.8$ s^{-1}. The above results along with those of the other scenarios are summarized in Table 1.

The maximum possible surface energy fluxes $e_{\max}$ do not provide practical estimates for determining the thermal effect on ice/snow melt/accumulation, because large amounts of the dissipating heat do not reach the icy road (heat exchanged between the vehicle body and the air is largely convected away from the road surface). However, if only a small fraction of this heat affects the road ice deposit, the corresponding effect on ice melting or suppression of road freeze conditions when the background air temperature is ≈0°C is still likely to be significant. In the ULS scenario, 7% of $e_{\max}$ amounts to ~100 W m^{-2}, which would offset the clear-sky net longwave radiation flux cooling that would occur without traffic (see section 3). In the following sections, we analyze each of the processes 1–5 listed in the beginning of section 1 to estimate more precisely the true thermal energy flux into the road surface. Figure 2 provides a schematic illustration of the various vehicle heat sources evaluated in this paper.

We begin by breaking the overall energy flow into several components. Each component may then be analyzed in detail to estimate better its contribution to actual road surface flux. One such component is the thermal energy flow generated by dissipation of mechanical energy E_m. Other direct thermal energy losses are due to radiation and heat convection from the hot surfaces of the engine, cooling, and exhaust pipe systems, denoted by E_e, E_c, and E_p, respectively. Energy may also be lost because of irreversibilities in the combustion process, denoted by E_{comb}. The overall model energy balance is

$$E_{\text{tot}} = E_m + E_e + E_c + E_p + E_{\text{comb}}. \qquad (2)$$

b. *Thermal contribution of dissipated mechanical energy*

The total engine energy generation rate E_{tot}, along with the total mechanical power E_m, developed by the IC engine in each driving scenario is presented in Table 2. The magnitudes of E_m and the engine efficiency E_m/E_{tot} were estimated from knowledge about the magnitudes of mechanical loss terms, as well as engine efficiency trends presented in Heywood (1988). In the ULS scenario we estimated $E_m = 8.6$ kW. The estimate of

TABLE 2. Overall vehicle energy flow statistics (kW).

Parameter $E_{(\ )}$	Driving scenario			
	Urban stopped traffic (UST)	Urban heavy snow (UHS)	Urban light snow (ULS)	Highway light snow (HLS)
[a]Total engine energy generation rate E_{tot}	22	49	49	90
Energy components				
Mechanical power E_m	2.7	8.6	8.6	31.0
Engine exhaust enthalpy E_p	6.7	14.6	14.6	26.7
[b]Engine coolant heat transfer E_c	10.9	21.2	20.5	23.2
Direct engine thermal loss E_e	0.6	2.1	2.8	4.6
[c]Combustion losses E_{comb}	1.1	2.5	2.5	4.5

[a] Assumes perfect combustion with the theoretical amount of air.
[b] Determined from overall energy balance on engine ($E_c = E_{tot} - E_m - E_p - E_e - E_{comb}$).
[c] Assumed to be 5% of E_{tot} (Heywood 1988).

the value of E_m for the UST scenario required special treatment. A series of polynomial fits to the IC engine efficiency estimated at nonzero speeds was used to determine its limiting value as $V \to 0$.

The mechanical energy dissipates (ignoring changes in the potential energy of the vehicle) into heat because of rolling frictional losses, aerodynamical drag, and other secondary loss processes (power train losses, braking losses, and losses in vehicle accessories), denoted by E_f, E_d, and E_o respectively. Thus,

$$E_m = E_f + E_d + E_o. \tag{3}$$

The first term on the rhs of Eq. (3), E_f, generates an immediate and concentrated thermal heat release at the road surface, whereas the second term, E_d, generates heat throughout a relatively large volume of air surrounding the vehicle (termed henceforth as the dissipative air mass and denoted DM; see Fig. 3 for illustration). Only a fraction of the dissipated turbulence energy reaches the road surface. The secondary losses represented by the third term, E_o, also contribute to additional convective and radiative fluxes reaching the ground from the vehicle. In the following, the magnitudes of these three components are evaluated.

1) CONTRIBUTION FROM ROLLING FRICTION

Frictional losses associated with rolling tires have an obvious, observable effect on ice melt. The frictional loss rate for a single moving vehicle is

$$E_f = \mu m_v g V, \tag{4}$$

where μ is the rolling friction coefficient, m_v is the vehicle mass, and g is the acceleration of gravity. The value of μ depends on the tire (type, load, and condition) as well as on the depth and the mechanical properties of the accumulated icy deposit on the road. These dependencies are proprietary and have not been reported in the open literature. We have determined a representative value $\mu \approx 0.01$ for our model vehicle on dry pavement by measuring the distance ΔX required for the vehicle to coast to a stop on a flat road given an initial velocity V. By assuming that μ is constant and the speed is low enough that aerodynamic drag (or any other mechanical loss term) is not a factor, a straightforward integration of Eq. (4) and equating the result to the initial vehicle kinetic energy yields the expression $\mu = V^2/(2g\Delta X)$. For a nonuniform layer of compacted snow and ice, however, there is considerably more surface roughness and contact with the tire, which substantially increases the value of μ. Application of ice-melting chemicals also tends to increase the rolling friction coefficient. Thus for heavy snow/ice surface conditions, we assume that $\mu \sim 0.05$.

By denoting W_t (~0.2 m) as the width of a tire, the quasi-steady surface thermal flux owing to frictional loss of many vehicles moving over the same two tire tracks is

$$e_f = \frac{\alpha_f E_f}{2W_t(L + S)}, \tag{5}$$

where $0 \le \alpha_f \le 1$ is the fraction of the frictional loss directly affecting the road surface. Given the moving traffic parameters listed in Table 1 and with the assumption that $m_v \sim 1000$ kg, in the UHS scenario $E_f = 5.0$ kW (see Table 3). With the assumption that an extreme case of $\alpha_f = 1$, then $e_f = 0.4$ kW m^{-2}. Additional factors to be accounted for are (i) variations in tire width dependent on vehicle type and double tires for large vehicles and (ii) successive vehicle's tire tracks not overlapping. Considering these effects, we replace W_t in Eq. (5) with an equivalent width of traction $W_{eq} = W_v/2$. Then if $\alpha_f = 1$, the heat flux from rolling friction loss is $e_f = 98$ W m^{-2} for scenario UHS.

Somewhat more refined estimates for α_f can be made by considering fluxes into the nearby air and road surface. Several measurements that we made when the air temperature was ≈0°C and immediately after a drive (long enough for the tire to reach steady state) indicate an excess tire external surface temperature on the order of 5°C. This temperature is sufficiently high to allow up to 1 kW of convective heat transfer from the tires to the ambient atmosphere in the moving scenarios. This estimate was based upon the excess tire temperature,

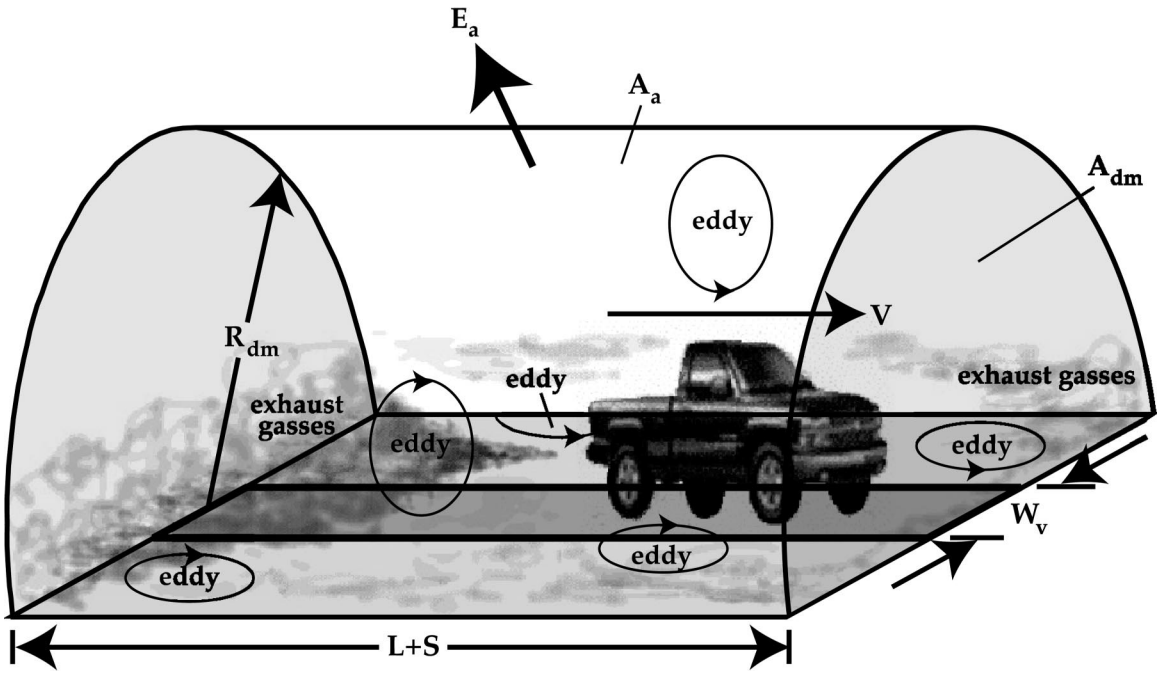

FIG. 3. Schematic illustration of the vehicle and its surrounding DM. The aerodynamic drag of the vehicle energizes turbulent mixing in the DM, depicted here by the formation of numerous eddies (of characteristic size l_{eddy}). Thermal radiative fluxes from the vehicle are directed into the road surface primarily in the central strip (darkened). Thermal convective fluxes from the vehicle are conveyed into the DM primarily through a boundary layer under the vehicle. These convective fluxes are then conveyed to the road surface and the ambient environment via the turbulent mixing in the DM. Direct radiative exchange also occurs between the road surface and the sky. For the notation legend, see the text.

tire surface area, and the outer convection heat transfer coefficient h_o [see section 2c(1) below, and Table 5]. Modeling of the road bed as a semi-infinite solid with an oscillating surface temperature (Stokes's second problem; White 1991) indicates that the thermal boundary layer in the road bed is $\sim 0.4\sqrt{\kappa_{road}/f}$ (e.g., $\sim$0.3 mm thick for the moving scenarios, where the road thermal diffusivity κ_{road} is 1.0×10^{-7} m^2 s^{-1} for asphalt and 6.5×10^{-7} m^2 s^{-1} for concrete). Although this is very small and indicates that any heat in the tires not convected away may be efficiently conducted into the pavement, it is offset by the small contact area of the

TABLE 3. Computed vehicle energy loss paths (kW).

Parameter $E_{(\ )}$	Driving scenario			
	Urban stopped traffic (UST)	Urban heavy snow (UHS)	Urban light snow (ULS)	Highway light snow (HLS)
Mechanical losses				
Rolling friction loss E_f	0	5.0	1.5	3.0
[a] Aerodynamic drag loss E_d	0	0.7	2.5	19.7
[b] Other losses E_o	2.7	2.9	4.6	8.3
[c] Exhaust losses				
Convective loss E_{cp}	1.2	8.1	9.6	18.8
Radiative loss E_{rp}	4.5	4.5	3.4	4.3
Exit enthalpy E_{ex}	1.0	2.1	1.6	3.5
Direct engine losses				
Convective loss E_{ce}	0.3	1.8	2.5	4.3
Radiative loss E_{re}	0.3	0.3	0.3	0.3

[a] Computed from Eq. (6) with $C_d \sim 0.42$ (following Munson et al. 1990) and $A_d \sim 2.7$ m^2 as representative values of vehicle drag coefficient and cross-sectional area, respectively; $\rho_a = 1.29$ kg m^{-3} is the ambient atmospheric density.

[b] Includes mechanical energy losses other than aerodynamic drag and following friction (e.g., power train, braking, accessories). Value determined via mechanical energy balance ($E_o = E_m - E_f - E_d$).

[c] Computed using exhaust system model (appendix A).

TABLE 4. Computed turbulence parameters of the dissipative air mass. See sections 2b(2) and 4b for formulation.

Parameter	Driving scenario			
	Urban stopped traffic (UST)	Urban heavy snow (UHS)	Urban light snow (ULS)	Highway light snow (HLS)
Dissipation rate $\varepsilon_{\text{eddy}}$ (W kg^{-1})	—	3.5	41	20
Eddy velocity u_{eddy} (m s^{-1})	—	1.5	3.4	2.5
Eddy kinematic viscosity ν_{eddy} (m^2 s^{-1})	—	0.11	0.24	0.18
DM radius R_{dm} (m)	—	1.8	1.2	3.3
Eddy dissipation timescale τ_{eddy} (s)	—	0.7	0.3	0.4
Convection timescale τ_{conv} (s)	—	3.0	1.3	1.8

tires with the road ($\sim$0.05 m^2). We conclude that for the ULS and HLS scenarios most of the rolling friction loss is convected away into the ambient air and only a fraction ($\alpha_f \sim 0.25$) is deposited into the road surface. However, for the UHS scenario, because of enhanced tire contact with the snow/ice layer, a larger fraction ($\alpha_f \sim 0.5$) is assumed. Through Eq. (5), the corresponding values of e_f for the urban heavy-snow and light-snow driving scenarios are 49 and 11 W m^{-2}, respectively.

2) CONTRIBUTION FROM AERODYNAMIC DRAG

The mechanical energy loss from aerodynamic drag is

$$E_d = F_d V, \tag{6}$$

where $F_d = 0.5 C_d \rho_a A_d V^2$. Here A_d and C_d are the vehicle cross-sectional area and drag coefficient, respectively, and are given in Table 3, and ρ_a is the ambient air density. In the UHS case, $E_d = 0.7$ kW. This energy flow ultimately is dissipated away completely into heat via molecular viscosity acting upon the smallest scales of turbulent motion in the DM. An estimate of the fraction of E_d that ultimately reaches the road surface requires a global energy balance on the DM. Additional terms beyond E_d needed for this balance are evaluated later in section 4, and thus further details are not presented here. However, estimates of the turbulent scales in the DM transport processes are based only upon the aerodynamic drag forcing of the vehicle on the DM and are developed in the following paragraph.

The volume of the DM is $V_{\text{dm}} = A_{\text{dm}}(L + S)$, where A_{dm} is its cross-sectional area. For free turbulent wakes, A_{dm} is velocity independent. However, the spacing and vehicle size in this study force external scales upon the flow, which modify this result. The road surface also introduces a boundary layer aspect; thus, the value of A_{dm} may depend upon A_d, L, S, and V. As a first approximation for the UHS scenario, we assume that $A_{\text{dm}} \sim 2A_d$, and thus $V_{\text{dm}} \sim 160$ m^3 for this case. Based upon this volume and the drag loss rate, the turbulent energy dissipation rate (energy loss rate per unit mass in the DM) is $\varepsilon_{\text{eddy}} \sim E_d/(\rho_a V_{\text{dm}}) = 3.5$ W kg^{-1}. From $\varepsilon_{\text{eddy}} \sim u_{\text{eddy}}^3/l_{\text{eddy}}$ (Tennekes and Lumley 1972) it then follows that $u_{\text{eddy}} \sim 1.5$ m s^{-1} for $l_{\text{eddy}} \sim 1$ m (set by the vehicle cross-sectional area). Here l_{eddy} and u_{eddy} are the characteristic size and velocity of the largest eddies in the DM. The timescale for dissipation is given by the eddy turnover time, $\tau_{\text{eddy}} \sim l_{\text{eddy}}/u_{\text{eddy}}$. For the UHS scenario, $\tau_{\text{eddy}} = 0.7$ s. The convective timescale is directly related to the vehicle motion (in the absence of wind) and is $\tau_{\text{conv}} \sim (S + L)/V = 3.0$ s. Values of these parameters for all the driving scenarios are summarized in Table 4. Because for all relevant driving scenarios the eddy turnover time is smaller than the convective timescale, the drag loss will be converted into heat quickly enough that it can be a significant source of heating to the DM around the vehicle.

3) CONTRIBUTION FROM OTHER MECHANICAL LOSSES

The final category of mechanical losses, E_o, involves secondary processes such as drivetrain losses, braking losses, and so on. Modern drivetrains are very efficient, with transmissions transferring close to 100% of the mechanical power at highway road speeds. This efficiency contrasts with the stopped-traffic scenario, in which drivetrain losses account for 100% of the mechanical power loss. Braking losses are significant only for the urban driving scenarios. The magnitudes of these losses are determined from a mechanical energy balance ($E_o = E_m - E_f - E_d$) and are listed in Table 3. Given that the drivetrain and brake housings face into the interior region below the body of the vehicle, these losses contribute to a radiative road surface thermal flux. For the ULS scenario, $E_o = 4.6$ kW. To estimate what fraction of this energy reaches the road surface, it is necessary to break it down into radiated and convected components. The ratio of net radiative to convective energy transfers may be estimated as $R \sim 4\varepsilon\sigma T_a^3/h_o$ where ε is the radiative surface emissivity, σ is the Stefan–Boltzmann constant, T_a is the ambient temperature, and h_o is the outer convection coefficient. Then the fraction of other mechanical losses that is radiated into the road surface is $\alpha_o = R/(1 + R)$. This approximation assumes that $\Delta T/T_a \ll 1$, where ΔT is the enhancement in surface temperature above the ambient for vehicle parts affected by these losses. For dirty radiative surfaces, which are typical, $\varepsilon \sim 1$. Given $h_o = 50$ W m^{-2} K^{-1} [see section 2c(1) below, and Table 5], for the ULS scenario 8.5% or 0.4 kW of E_o would be transferred by radiation into the road surface, and the remaining

TABLE 5. Thermodynamic/heat transfer parameters.

Parameter	Driving scenario			
	Urban stopped traffic (UST)	Urban heavy snow (UHS)	Urban light snow (ULS)	Highway light snow (HLS)
[a]Outer convection coefficient h_o (W m^{-2} K^{-1})	5	35	50	85
Road surface convection coefficient h_{road} (W m^{-2} K^{-1})	5	8	12	15
Equivalent eddy convection coefficient h_a (W m^{-2} K^{-1})	5	75	250	68
[b]Equivalent radiative convection coefficient h_r (W m^{-2} K^{-1})	19	19	18	19
Fraction of rolling friction loss directed into road surface α_f	—	0.5	0.25	0.25
[b]Fraction of other mechanical loss directed into road surface via radiation α_o	0.3	0.12	0.085	0.05
Exhaust system exit temperature T_{exe} (°C)	101	100	77	94
Combustion products mass flow rate $\dot{m}_{\text{ex}}$ (kg s^{-1})	0.0081	0.0177	0.0177	0.0323
[c]Fraction of exhaust vapor that condenses α_{cond}	0	0	0.6	0
Exhaust exit condensation E_{cond} (kW)	0	0	2.3	0
[d]DM mean temperature T_{dm} (°C)	5.0	2.8	2.2	1.9

[a] Computed from Eq. (9) assuming the smooth skin friction coefficient C_f is increased 30% by surface roughness.
[b] UST value is nonequilibrium (see section 4c).
[c] Computed using one-dimensional differential condensation model with ~0.2-μm particles and a particle mass fraction (relative to $\dot{m}_{\text{ex}}$) of 0.0001.
[d] Prescribed for UST.

91.5% would be transferred by convection into the DM surrounding the vehicle. We denote the radiative component as $\alpha_o E_o$, with $\alpha_o = 0.085$ in the current driving scenario (with $0 \leq \alpha_o \leq 1$). For the UST scenario, the equilibrium value (see section 4c) is $\alpha_o = 0.48$, yielding $\alpha_o E_o = 1.3$ kW (see Table 5 for data on the other scenarios). The corresponding convective fluxes are $(1 - \alpha_o)E_o$.

c. IC engine, exhaust system, combustion, and coolant system thermal losses

The difference between E_{tot} and $(E_m + E_{\text{comb}})$ listed in Table 2 gives the thermal loss rate E_t in the IC engine as 37.9 kW for the ULS scenario (see Fig. 4). A large fraction of this lost power goes into the enthalpy of the combustion products E_p. These products exit the engine at $T_{\text{exi}} \sim 980$ K (Heywood 1988) and thus carry a very large sensible heat (14.6 kW) in the ULS scenario. Results from the exhaust system thermal analysis follow below, and the exhaust system model is outlined in appendix A. An assumption that combustion losses (E_{comb}, from chemical irreversibilities) typically amount to about 5% of E_{tot} (Heywood 1988) yields $E_{\text{comb}} \sim 2.5$ kW. Direct thermal losses E_e from the engine amount to about 2.8 kW in the ULS scenario (see next section for computation). This leaves 20.5 kW of waste heat E_c to be removed from the engine by the cooling system [see Eq. (2)]. These energy loss rates are summarized in Table 2 for each of the driving scenarios.

1) CONTRIBUTION OF DIRECT THERMAL LOSSES FROM ENGINE

We assume that the heated engine's bottom surfaces can be represented as an equivalent horizontal surface of area A_e and temperature T_e. The net longwave irradiance loss from the engine surface is

$$E_{\text{re}} = \sigma A_e (T_e^4 - T_{\text{road}}^4), \tag{7}$$

where $T_{\text{road}}(\approx 0°\text{C})$ is the road surface temperature and the surface emissivity has again been assumed to be $\varepsilon \sim 1$ (the effect of lower emissivity values is evaluated in section 5b). Although exact values of A_e and T_e are difficult to pin down (T_e is highly variable over the engine surface area A_e), direct observations with an IR radiometer and temperature thermocouple suggest $T_e \sim 50°\text{C}$ as a reference level over an area $A_e \sim 1$ m^2. These values yield a maximum net downward irradiance from the engine surface of $E_{\text{re}} = 0.3$ kW. The convection heat transfer from this equivalent surface is

$$E_{\text{ce}} = h_o A_e (T_e - T_a), \tag{8}$$

which yields, for the ULS scenario, $E_{\text{ce}} = 2.5$ kW. The direct thermal loss from the engine is given by $E_e = E_{\text{re}} + E_{\text{ce}}$.

The outer convection coefficient h_o is computed using the Nusselt number correlation (Schlichting 1979)

$$\text{Nu}_o = (C_f/2)\text{Re}_o \text{Pr}_a^{1/3}, \tag{9}$$

where $\text{Nu}_o = h_o l_v / k_a$, l_v is a characteristic length for the vehicle and k_a is the thermal conductivity of the air; $\text{Re}_o = l_v V/\nu_a$ is the Reynolds number and ν_a is the kinematic viscosity of the air; $\text{Pr}_a = \nu_a/\kappa_a$ is the Prandtl number and κ_a is the thermal diffusivity of the air; and C_f is the skin friction coefficient. Using $l_v \sim L$ and a film temperature of ~300 K, the ULS scenario yields $\text{Re}_o = 4.7 \times 10^6$. For smooth surfaces, $C_f = 0.074\text{Re}_o^{-1/5}$ and $\text{Nu}_o = 7200$, yielding $h_o = 38$ W m^{-2} K^{-1}. For rough surfaces as found under the car, the friction and hence convection coefficients may be enhanced, so the

values of h_o shown in Table 5 have been increased by ~30% relative to smooth surface values.

2) CONTRIBUTION OF DIRECT THERMAL LOSSES FROM EXHAUST SYSTEM

The net radiative loss from the piping in the exhaust system is given by

$$E_{\text{rp}} = h_r A_p (T_{\text{pw}} - T_{\text{road}}), \tag{10}$$

where h_r is the equivalent radiative convection coefficient and A_p is the effective surface area of the piping in the exhaust system (see appendix A for definitions). Along with h_r, the average pipe wall temperature T_{pw} may be estimated using a parallel-mode radiation–convection analysis (see appendix A for details). The result is that, for the ULS scenario, $E_{\text{rp}} = 3.4$ kW. This energy is primarily directed down into the roadway. There is also significant thermal loss via convection, amounting to 9.6 kW in the current driving scenario, which may be computed from

$$E_{\text{cp}} = h_o A_p (T_{\text{pw}} - T_a). \tag{11}$$

These energy losses and those computed for the other driving scenarios are presented in Table 3.

3) THERMAL LOSSES ASSOCIATED WITH COMBUSTION AND COOLANT SYSTEM

All that remains to be considered are the road surface thermal fluxes associated with combustion losses and convection from the coolant system (the coolant system presents negligible surface area, and hence radiation, to the road surface). Combustion losses E_{comb} simply lower the amount of thermal energy being generated by the engine, resulting in unburned fuel being passed out in the exhaust gases. In this case there is no thermal energy term to consider. The convection of heat from the cooling system to the DM in the ULS scenario amounts to $E_c = 20.5$ kW. This is a significant source of thermal energy, the effect of which (along with other convective terms) on road surface flux is termed indirect exchange and is estimated in section 4 below.

3. Evaluation of net radiative flux into the road surface

The net effective radiative flux into a unit area of the icy road surface (confined to the road section over which vehicles travel, i.e., the inner area in Figs. 1 and 3) is

$$e_r = \frac{(\alpha_o E_o + E_{\text{re}} + E_{\text{rp}}) + (e_{\text{rd}} - e_{\text{ro}}) W_v S}{W_v (L + S)}, \tag{12}$$

where e_{rd} is the downwelling longwave atmospheric radiation flux, and $e_{\text{ro}} = \sigma T_{\text{road}}^4$ is the upwelling flux (radiated by the road surface) assuming a road surface emissivity of unity. In the derivation of (12), additional assumptions used are that (i) the nonheated bottom surfaces of the vehicle are at temperatures less than 20°C, making their radiative contribution approximately balanced by the road upwelling IR flux—that is, they have a net ~0 W m^{-2} radiative flux; (ii) all radiative fluxes emitted by the exhaust pipe system, engine, and other radiative sources ultimately end up striking the road surface under the vehicle; (iii) longwave radiation contributions into the road surface not under the vehicle are considered secondary and not included; and (iv) nighttime or heavily overcast daytime conditions are present, and thus shortwave radiation effects are omitted. The value of e_{rd} can be estimated following the method of Swinbank (1963) for a clear-sky situation (as would be the likely case for ideal freeze conditions) as

$$e_{\text{rd}} = 9.37 \times 10^{-6} \sigma T_a^6 \text{ (W m}^{-2}\text{)}. \tag{13}$$

For $T_a \approx 273$ K, $e_{\text{ro}} = 315$ W m^{-2}, and $e_{\text{rd}} = 220$ W m^{-2}, and so for the HLS scenario the net flux of IR radiation into the road surface is $e_r = -33$ W m^{-2}. This value, when compared with $e_r = e_{\text{rd}} - e_{\text{ro}} = -95$ W m^{-2} (which is obtained assuming the absence of any traffic), yields an effective gain in net radiative flux of 62 W m^{-2}. For the case of stopped traffic with reduced spacing, the effect is much more dramatic, with equilibrium value (see section 4c) $e_r = 410$ W m^{-2} and a net IR flux gain of 505 W m^{-2}.

When the sky is cloudy, as would be the case under snowfall conditions, the Paltridge and Platt (1976, p. 140) relation may be adopted. For low-level clouds (which were assumed in the current study), it gives the downwelling radiation flux e_{rdc} as a function of cloud fraction of the sky c:

$$e_{\text{rdc}} = e_{\text{rd}} + 0.3 \sigma c T_c^4, \tag{14}$$

where T_c is the cloud-base temperature (assuming unit emittance of the cloud). In a completely overcast sky ($c = 1$) with $T_c \approx T_a$ (i.e., isothermal lower atmosphere) the HLS case yields $e_r = 53$ W m^{-2} and the UST case yields an equilibrium value (see section 4c) $e_r = 450$ W m^{-2}. In contrast, under these meteorological conditions without any traffic, $e_r \approx 0$ W m^{-2}. Results for e_r in clear and overcast conditions for all driving scenarios are summarized in Table 6.

The values of the various radiative fluxes estimated in the previous two paragraphs are based upon an emissivity of ~1 for hot vehicle surfaces. This value is an upper limit but is expected to be realistic for dirty surfaces (i.e., those covered with oxidation layers, dirt, and/or oil).

4. Indirect and direct heat exchange between the vehicle, air, and road surface

By indirect exchange we refer to the convective exchange between the vehicle body and the DM through (i) convection between the warm surfaces of the vehicle body to the DM, (ii) hot exhaust gas emissions, and (iii) aerodynamic drag [see section 2b(2)]. Direct heat ex-

TABLE 6. Contributions to net road surface fluxes (W m^{-2}).

Parameter $E_{(\ )}$	Driving scenario			
	Urban stopped traffic (UST)	Urban heavy snow (UHS)	Urban light snow (ULS)	Highway light snow (HLS)
Rolling friction e_f	0	49	11	8
*Net radiative flux e_r: clear sky	377	22	49	−33
(overcast sky)	(412)	(100)	(120)	(53)
Downward road surface flux due to direct exchange e_{road}	25	22	35	19
*Net road surface flux with clear sky e_{net}: inner	400	93	95	−6
(outer)	(−70)	(−73)	(−60)	(−76)
*Net road surface flux under overcast sky e_{net}: inner	435	171	166	80
(outer)	(25)	(22)	(35)	(19)

* UST value is nonequilibrium and does not consider intermittency (see section 4c). To illustrate the computation of the effect of intermittency, suppose $\tau_{mov} = 0.5$ and the moving scenario is UHS. Then, for stop-and-go traffic, the direct flux is $e_{road} = 23.5$ W m^{-2} and the radiative fluxes are $e_r = 200$ and 256 W m^{-2} for clear and overcast skies, respectively. Then the net inner road surface fluxes are $e_{net} = 247$ and 303 W m^{-2} for the clear and overcast skies, respectively.

change refers to sensible heat flux between the DM and the road surface.

a. Indirect heat exchange

1) CONTRIBUTION FROM VEHICLE THERMAL CONVECTION

The vehicle convection contribution consists of several components: convective heat exchange along the surfaces of the tires from rolling friction loss $(1 - \alpha_f)E_f$, other components associated with mechanical losses (drivetrain, brakes, etc.) $(1 - \alpha_o)E_o$, and direct thermal losses from engine E_{ce}, cooling system E_c, and exhaust pipe systems E_{cp}. Thus

$$E_{conv} = (1 - \alpha_f)E_f + (1 - \alpha_o)E_o + E_{ce} + E_c + E_{cp}. \quad (15)$$

For the ULS scenario, the total convective exchange sums to $E_{conv} \approx 38$ kW per moving vehicle (see Table 7).

2) CONTRIBUTION FROM EXHAUST GAS EMISSIONS

The mass flow rate and temperature of gases emitted from the exhaust system of the model vehicle are listed in Table 5. For the ULS scenario, $\dot{m}_{ex} = 0.0177$ kg s^{-1} and $T_{exe} = 77$°C, respectively (these values are determined from the combustion and exhaust system models, appendices B and A, respectively). Using

$$E_{ex} = \dot{m}_{ex} c_{pex}(T_{exe} - T_a), \quad (16)$$

the exhaust gases deliver an additional 1.6 kW of sensible heat to the air (see Tables 3 and 5). Although these gases are buoyant, there is significant mixing into the DM with a concomitant increase in DM temperature. Here c_{pex} is the specific heat of the combustion products, where its value is based upon the composition of the products and their logarithmic mean temperature (LMT). In the ULS scenario, LMT = 285°C and $c_{pex} = 1.16$ kJ kg^{-1} K^{-1}.

Another possible source of heat for the DM mixing volume around the vehicle is related to condensation of water vapor in the exhaust,

$$E_{cond} = \alpha_{cond} m'_{H_2O} \dot{m}_{ex} \lambda_{fg}, \quad (17)$$

where $m'_{H_2O}(=0.089)$ is the water vapor mass fraction in the exhaust system (see appendix B), α_{cond} is the fraction of water vapor that condenses, and $\lambda_{fg}(=2.50$ MJ kg$^{-1})$ is the latent heat of condensation of water vapor. Maximum effects are achieved with $\alpha_{cond} = 1$.

TABLE 7. Computed net energy transfer rates (kW). UST values are nonequilibrium (see section 4c).

Parameter $E_{(\ )}$	Driving scenario			
	Urban stopped traffic (UST)	Urban heavy snow (UHS)	Urban light snow (ULS)	Highway light snow (HLS)
Total energy flow into the DM E_{dm}	15.3	38.0	44.4	79.6
Total thermal energy convected E_{conv}	14.3	36.2	37.9	56.4
*Total energy loss to the ambient air E_a	14.8	36.6	42.7	72.7
**Net road surface energy flow under clear sky E_{net}	4.9	0.3	2.3	−21
	(22% of E_{tot})	(0.6% of E_{tot})	(5% of E_{tot})	(−23% of E_{tot})
**Net road surface energy flow under overcast sky E_{net}	6.1	10.0	6.1	12.7
	(28% of E_{tot})	(20% of E_{tot})	(12% of E_{tot})	(14% of E_{tot})

* The UST value is computed from $E_a = E_{dm} - A_{road}e_{road}$ instead of Eq. (20) because the DM analysis for T_{dm} is inappropriate in this scenario.

** The UST values are nonequilibrium; see section 4c.

An improved estimate of α_{cond} requires consideration of nonequilibrium thermodynamics, the turbulent mixing of exhaust gases with the ambient atmosphere in the DM, and the distribution of particulates in the exhaust stream, which provide condensation nuclei for the water vapor. We employed a one-dimensional differential condensation model (based upon the turbulent jet) to estimate the values of α_{cond} and E_{cond} for the various driving scenarios (values are presented in Table 5). Typical values of α_{cond} have only a marginal effect on sensible heat flux exchange between the DM and road surface (see later section 5b).

b. Direct heat exchange between the DM and the road surface

The heat flux between the DM and the road surface may be estimated as

$$e_{road} = h_{road}(T_{dm} - T_{road}), \tag{18}$$

where h_{road} is the convection coefficient along the road surface, and T_{dm} is the DM mean temperature. Procedures to evaluate h_{road} and T_{dm} follow.

The boundary layer under the moving vehicle typically never reaches the road until well after the passage of the vehicle, and as a result $h_{road} < h_o$. For example, the 15 m s^{-1} velocity of the ULS scenario results in a turbulent boundary layer under the vehicle that is ~0.1 m thick [$\delta \sim 0.4L\mathrm{Re}_o^{-1/5}$, where δ is the boundary layer thickness at the back end of the vehicle and Re_o is the outer Reynolds number (Schlichting 1979)]. The typical distance from the road surface to the vehicle undercarriage is ~3 times as large. To estimate h_{road}, we use correlation Eq. (9) using u_{eddy} and $R_{dm} = \sqrt{2A_{dm}/\pi}$ (assuming a semicylindrical DM as illustrated in Fig. 3) as the velocity and length scales [see 2b(2)].

The mean temperature T_{dm} of the DM surrounding the vehicle may be estimated using the following energy balance:

$$E_{dm} = A_{road}e_{road} + E_a, \tag{19}$$

where $E_{dm} = E_{conv} + E_{ex} + E_{cond} + E_d$ is the total energy flowing into the DM, $A_{road} = 2R_{dm}(L + S)$ represents the area of road undergoing thermal exchange, and

$$E_a = h_aA_a(T_{dm} - T_a) \tag{20}$$

represents enthalpy lost to the ambient air through the outer surface of the DM, with $A_a = \pi R_{dm}(L + S)$ being the area of this outer surface and h_a being an equivalent convection coefficient along it. Here E_a is estimated using the Reynolds (heat/momentum) analogy [Eq. (9)] to derive the approximation $h_a \sim \rho_a c_p \nu_{eddy}/R_{dm}$. The eddy kinematic viscosity ν_{eddy} is estimated using τ_{ave}, the average shear stress along the boundary of the DM (determined via the global momentum balance $\tau_{ave} \sim 0.5F_d/A_a$), according to $\nu_{eddy} \sim \tau_{ave}l_{eddy}/(\rho_a u_{eddy})$. The eddy scales are assumed to satisfy the mixing length result $\nu_{eddy} \sim \Omega l_{eddy}u_{eddy}$, (Schlichting 1979; White 1991), where Ω is a universal constant. Consistency among all eddy parameters (ε_{eddy}, l_{eddy}, u_{eddy}, and ν_{eddy}) requires that $R_{dm} \sim S^{0.88}$ (with no dependency of R_{dm} upon V)—the selection of $R_{dm} \sim 1.8$ m for the UHS scenario [see section 2b(2)] results in $\Omega \sim 0.07$. Assuming $T_{road} \approx T_a$ in Eq. (18) and substituting Eqs. (6), (15)–(18), and (20) into Eq. (19) leads to an equation for T_{dm}. With T_{dm} determined, Eq. (18) yields the direct heat flux into the road surface. Values for all required parameters may be found in Tables 3–5.

For the ULS scenario, we find $R_{dm} = 1.2$ m, $\nu_{eddy} = 0.24$ m^2 s^{-1}, $h_a = 250$ W m^{-2} K^{-1}, and $h_{road} = 16$ W m^{-2} K^{-1}. The corresponding DM bulk temperature and surface road flux are $T_{dm} = 2.2$°C and $e_{road} = 35$ W m^{-2}, respectively. Results for the driving scenarios UHS and HLS are given in Tables 5–7.

c. The stopped-traffic scenario UST

The method for determining the exchange coefficients in the previous section is based upon the use of a global momentum balance to determine the size of the DM. It is inappropriate to use it when $V \to 0$. Another complication in this scenario is that the radiative energy flow is not in equilibrium; that is, vehicles stopped in traffic are likely to have just stopped (for a traffic signal) and so are reacting to sudden and large changes in h_o. Put another way, the UST equilibrium energy flow only results when vehicles are stopped for a very long time. The net effect of this transience is that the vehicle contributions to the radiative fluxes e_r predicted by Eq. (12) will be too large (emitting surfaces will be warming up to equilibrium values in response to the sudden decrease in convection).

In this scenario, we assume the following: (i) all heat transfer coefficients are due to calm winds, and thus $h_o \sim h_{road} \sim 5$ W m^{-2} K^{-1}; (ii) the DM temperature is $T_{dm} \sim 5$°C [T_{dm} cannot be computed via Eq. (19)]; (iii) $R_{dm} \sim W_v/2 + 0.5 = 1.4$ m; and (iv) the vehicle radiative emissions used to determine e_r [using Eq. (12)] are the average of scenario UHS and *equilibrium values* for UST (the latter are $\alpha_o = 0.48$, $E_{re} = 0.3$ kW, and $E_{rp} = 4.5$ kW, and thus $e_r = 413$ and 448 W m^{-2} for the clear and overcast skies, respectively). In particular, the radiative parameters appearing in Tables 5–7 for the UST scenario are not the equilibrium values but are instead values corrected for the *thermal unsteadiness* resulting from the *sudden* stopping of a vehicle. The equilibrium values for e_r are too large because typically a vehicle will resume motion (and hence experience the cooling effect of larger convection coefficients) before radiating surfaces have heated up to their equilibrium values.

A second kind of unsteadiness is relevant for the UST scenario because stopped traffic is intrinsically a transient phenomenon. That is, the nonequilibrium results for the UST scenario, shown in Tables 5–7, even though corrected (crudely) as above for nonequilibrium thermal

effects on the vehicle, still do not fully reflect nonequilibrium effects on the road surface. Consider a road intersection in which a traffic light stops traffic alternately between two directions (e.g., east–west vs north–south). We define an intermittency factor τ_{mov}, which is the fraction of time that traffic will be moving through the intersection. Then the average value of any thermal variable ϕ affecting the road surface may be approximated as $\tau_{mov}\phi_{mov} + (1 - \tau_{mov})\phi_{stop}$, where ϕ_{mov} and ϕ_{stop} are the corresponding values of the thermal variable for moving and stopped scenarios, respectively. For example, if $\tau_{mov} = 0.5$ and the moving scenario is UHS, then $e_r = 200$ and 256 W m^{-2} for clear and overcast skies, respectively.

5. Net thermal flux at the road surface

a. Formulation and computed values

The net thermal flux at the surface may be computed by adding together (i) the direct rolling friction loss e_f, (ii) the net radiative flux at the surface e_r, and (iii) the direct heat exchange e_{road}. By taking into account that different width scales have been employed (the vehicle width W_v for rolling friction and radiative flux vs the DM width $2R_{dm}$ for the direct heat exchange), the net downward flux may be computed as

$$e_{net} = \begin{cases} (e_f + e_r + e_{road}) & \text{over the inner area, } W_v(L + S) \\ (e'_r + e_{road}) & \text{over the outer area, } (2R_{dm} - W_v)(L + S), \end{cases} \quad (21)$$

and the total energy flow into the road surface is

$$E_{net} = (L + S)[W_v(e_f + e_r + e_{road}) + (2R_{dm} - W_v)(e'_r + e_{road})]. \quad (22)$$

For illustration of the inner and the outer areas, see Figs. 1 and 3. Note that the e_r term that appears in Eqs. (21) and (22) is as defined in Eq. (12). The term e'_r is the variant of e_r without traffic radiative effects. For the ULS scenario with overcast skies, $e_{net} = 166$ W m^{-2} over the inner area (which the vehicle passes directly over) and $e_{net} = 35$ W m^{-2} over the outer area (the vehicle does not pass directly over this area but it lies under the DM). The total energy flow is $E_{net} = 6.1$ kW, or 12% of the total energy generation rate of the IC engine. Results for the other scenarios are listed in Tables 6 and 7 (the intermittency factor τ_{mov} should be used in regions where traffic stops, as was outlined in the previous section). Note that the effect of cloud cover is very significant. With clear skies, the inner and outer fluxes drop to 95 and -60 W m^{-2}, respectively, and $E_{net} = 2.3$ kW for the ULS scenario.

Figure 4 shows an energy flowchart for the ULS scenario in clear-sky conditions. Direct thermal losses from the IC engine account for 77% of the energy flow. The dominant thermal terms are due to the cooling and exhaust systems, which together account for 72% of the energy flow. At higher speeds, aerodynamic losses become much more significant because they increase as $\sim V^3$. At lower speeds, all radiative effects become much more significant as all convective effects diminish. Note that 44 kW or 90% of the energy generated by the IC engine flows through the DM (this is E_{dm}). Ultimately 87% of the generated energy is lost to the ambient atmosphere. With cloudy skies, $A'_{road}e'_r$ is ≈ 0 W m^{-2} (where $A'_{road} = A_{road} - LW_v$), effectively increasing E_{net} by 3.8 kW (see Table 7).

b. The effect of change in some of the assumptions/parameters

In this section, the effects of changes in several assumptions and parameters on the thermal fluxes reaching the road surface are provided.

First the effect of a change in traffic density on the evaluated thermal fluxes reaching the road is explored. As a first approximation, it might be predicted that e_r [Eq. (12)] and e_{road} [Eq. (18)] would increase linearly with the decrease of traffic interval $(L + S)$, that is, $(e_r, e_{road}) \sim (L + S)^{-1}$. This elementary scaling was tested by running the model for modified ULS scenarios where $S = 25$, 35, 50, and 100 m were assumed. All other parameters remained the same as in the standard ULS scenario. The sensitivity of e_r to S matched precisely the above prediction for the overcast sky, in particular, $e_r \sim (L + S)^{-1.00}$ (note that $e'_r = e_{rd} - e_{ro} = 0$). For clear-sky conditions $(e_r + 95) \sim (L + S)^{-1.01}$ (where $e'_r = -95$ W m^{-2}). The direct flux into the road was also predicted well by the linear model, with $e_{road} \sim (L + S)^{-0.96}$.

The simplest approximation to the effect of vehicle speed on the thermal fluxes is to assume that e_r and e_{road} increase linearly with speed V. This would occur, for instance, if the net force acting on a moving vehicle remains constant (i.e., $E_{tot} \sim V$) and the radiative and direct thermal fluxes scale according to E_{tot}. The model was run for two modified HLS scenarios with $V = 10$ m s^{-1} (for which E_{tot} and E_m were 32 and 4.8 kW, respectively) and $V = 15$ m s^{-1} (for which E_{tot} and E_m were 49 and 8.6 kW, respectively). The standard and modified scenarios were used to determine that $e_{road} \sim V^{0.80}$—reasonably close to a linear estimate. However, the effect of V on the radiative fluxes was far from linear: for overcast skies, $e_r \sim V^{0.31}$; for clear skies $(e_r + 95) \sim V^{0.38}$.

Next, we consider the significance of the vehicle hot-surfaces emissivity ε and their area A on the thermal fluxes. Throughout our analysis, we have assumed unit surface emissivities in all radiative transfer computations. Although this assumption is appropriate for typical surfaces under typical driving conditions (e.g., they will be covered with dirt and oil and/or will be hot, which will tend to increase emissivities to close to 1), shiny metallic surfaces can have substantially lower

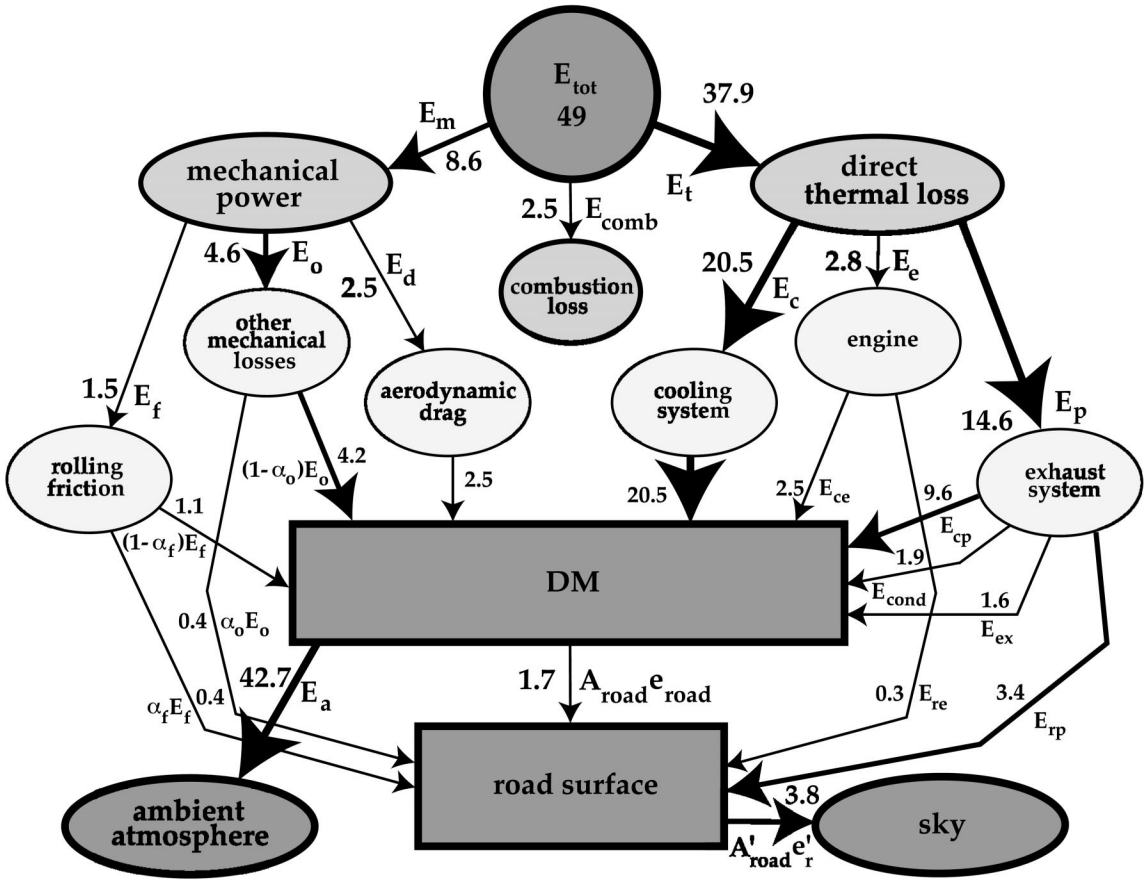

FIG. 4. Energy flowchart for the ULS scenario in clear-sky conditions. Particular values for the various energy rates appear in kilowatts near appropriate symbols but on opposite sides of the energy flow vector. Magnitudes of the flow vectors are approximately depicted by the sizes of the energy flow arrows and vector line thicknesses. The term E_t denotes the direct thermal loss from the engine ($E_c + E_e + E_p$).

emissivities. To gauge the extent of this effect, we computed the ULS scenario using $\varepsilon = 0.3$. This modifies the values of the following parameters: $\alpha_o = 0.03$, $E_{rp} = 1.3$ kW, $E_{cp} = 11.3$ kW, $E_{ex} = 2.0$ kW, $E_{re} = 0.1$ kW, and $e_r = -11$ and 60 W m^{-2} (clear and overcast skies, respectively). Assuming $\alpha_{cond} = 0.6$, the following parameters were then computed: $e_{road} = 37$ W m^{-2} and $e_r = -26$ and 44 W m^{-2} for clear and overcast skies, respectively. Overall, the effect of decreasing ε is an increase of only 5% in e_{road}, but a marked decrease of 75 W m^{-2} in radiative flux e_r. If the surface emissivity is 0.7, the decrease in radiative fluxes is 33 W m^{-2}. Thus the value of emissivity has a very strong, linear effect on model predictions for road surface radiative flux; that is, $\Delta e_r \sim \Delta\varepsilon$. Likewise, for the hot radiative surfaces, the areal change effect is expressed as $\Delta e_r \sim \Delta A$.

The fourth factor to be considered is the effect of the eddy length scale l_{eddy}. In section 2b(2) we assumed an $l_{eddy} \sim 1$ m based on the UHS scenario with $A_{dm}/A_d \sim 2$. This led to $\Omega \sim 0.07$ for the value of the universal constant used to determine the turbulence scales in the DM [see sections 2b(2) and 4b]. Here we consider the effect if $l_{eddy} \sim 2$ m instead, all other conditions being the same as scenario ULS. The universal constant decreases to $\Omega \sim 0.044$. Because the volume of the DM is assumed to be unchanged, this increases u_{eddy} and ν_{eddy} (because there is no change in ε_{eddy}). This enhanced turbulent mixing delivers more of the DM's excess thermal energy to the ambient atmosphere than to the road, with the net effect being that the direct road surface flux e_{road} drops 8 W m^{-2} (~25%) as compared with the standard ULS scenario described in the tables.

We conclude this section with an examination of the effect of exhaust vapor condensation α_{cond}. We computed the values of α_{cond} used in our scenarios [see section 4a(2)], but a sensitivity study revealed high sensitivity to the ambient relative humidity, the exhaust exit temperature, and the particulate distribution in the exhaust flow. Thus, it is likely that condensation fractions will show considerable variability. Using the ULS scenario as a base, a comparison of model runs with $\alpha_{cond} = 0$ and 1 showed an increase in the direct flux of e_{road} equal to 3.1 W m^{-2}, or about 9%. Thus, the sensitivity of e_{road} to the value of α_{cond} is secondary.

6. Discussion

The thermal energy generated by traffic was evaluated based on overall vehicle fuel consumption and its breakdown into relevant thermal components. The focus was made on heavy traffic scenarios associated with calm wind, which are conducive to enhancement of the net road thermal flux. Also a background temperature of $\approx 0^{\circ}$C was assumed for the air and the road. The complex nature of the processes involved requires for sake of simplicity the adoption of various assumptions and approximations in the parameterizations and models used. Although we have made every effort to determine and to use reasonable values for the various parameters, many are subject to variations of up to 50% or more from the nominal values used in this study. These variations are anticipated from two fundamentally different mechanisms: (i) stochastic variation of a parameter characteristic of a population of vehicles (e.g., emissivity of hot vehicle surfaces, kilometerage, drag coefficient, etc.)—this type of uncertainty primarily affects the data listed in Tables 1–3—and (ii) errors in the modeling approximations used to represent the relevant physical processes [e.g., turbulence model approximations in the DM as in sections 2b(2) and 4b, approximations on directionality of radiative fluxes from hot vehicle surfaces as in section 3, etc.]—these uncertainties more strongly affect the data listed in Tables 4–7. The data cited throughout the tables should be considered to be provisional.

Only a stochastic approach (i.e., using the current model, a very large number of examples could be studied) in parallel with refined observations of the mean values and low-order moments of these random parameters can fully determine the effects of stochastic variation. Such a concerted study is imperative in increasing the accuracy of future model evaluations. Uncertainties from model approximations can be reduced by the development of more exact models (e.g., the turbulence parameterizations used in our study could be replaced with numerical simulations of the turbulence in the DM, radiation exchanges between hot vehicle surfaces and the road surface could be precisely estimated using view-factor integrals, unsteady heat transfer analyses could be used to account more precisely for traffic periodicity and intermittency, etc.). With the current stochastic uncertainty in so many fundamental parameters, however, the development of more precise models is not warranted at this time.

Given these caveats, our results indicate that the net radiative fluxes from the vehicle's hot surfaces are the main traffic thermal contributors to the road surface heat balance. To the extent that the average emissivity of a population of vehicles is less than unity, our results for net radiative fluxes will be somewhat high. The value of $\varepsilon \sim 1$ is based upon ''dirty'' coatings over the vehicle hot radiative surfaces. Any cursory examination of typical vehicle undersides will show this to be a reasonable approximation. However, to the extent that these surfaces are clean or polished, emissivities as low as 0.2 are possible (we anticipate these very low values are most unlikely to be representative of a population mean value). Because the net thermal flux at the road surface is sensitive to the value of emissivity (see section 5b), the proper interpretation of our results are that the radiative fluxes are *most likely* the main traffic thermal contributors to the road surface heat balance.

One factor that has not been considered is surface wind. This will have more of an effect at higher wind speeds than at lower speeds, with the effect that oblique winds (i.e., winds blowing across the road) will blow the dissipative air mass away from the road surface and will decrease the convective fluxes into the road surface. To the extent that convection coefficients acting on vehicle surfaces are not substantially modified, radiative transfer processes will be unaffected (energy not convected must be radiated away; hence any change in convection coefficients will affect the radiative fluxes).

Under heavy traffic conditions, typical of urban and highway areas, it was found that the rolling friction loss contributions to positive thermal fluxes at the icy road surface are significant only if road conditions are such as to markedly increase tire friction coefficients above their nominal values on dry pavement (i.e., heavy snow conditions are required). On the other hand, radiative and convective heat exchanges between vehicles and the road surface are typically significant.

The concepts and formulation developed in this study to account for traffic thermal effects can be incorporated into or used in conjunction with operational forecast model predictions for surface temperature fields. This would allow an improved prediction of road snow/ice-layer conditions under heavy traffic situations, which would be of value and interest to the motoring public.

Validation of the formulation offered in this paper is an issue for a future research effort. It can be envisioned to be done qualitatively by evaluation of the increase in dry road skin temperature under a real traffic scenario. Such observations have been carried out in several of the studies cited in the introduction using remote IR sensing or temperature sensors placed at the road surface. For the purpose of validation, however, calibration of the characteristic traffic and vehicle parameters is needed. To focus on traffic radiative effects, a simplified controlled experiment can be designed in a parking lot for the urban stopped-traffic scenario. For example, representative vehicles travel in the area and stop for a measurement of the downwelling IR flux below the vehicle in comparison with that under open skies. In another parking lot experimental design, a given spot is considered as a ''traffic light'' and one (or more vehicles) stops in this spot in a frequency similar to that for a traffic light. The downwelling IR fluxes are then measured, as is the skin temperature of the pavement at the location of the vehicle stoppage. Measuring the substrate temperature would enable us to compute surface

pavement thermal flux and then through a heat balance equation to evaluate the surface sensible heat flux. Similar IR and temperature readings are also taken in other locations free of ''traffic,'' for comparison. This design would provide observational evaluation of traffic thermal effects, which can be used for additional validation of the formulation outlined in this paper.

Acknowledgments. The study was supported by NASA Grant NAG57561, Cooperative Program for Operational Meteorology, Education, and Training (COMET) Cooperative Agreement S0132791, the Department of Energy Climate Change Prediction Program, and the Iowa Department of Transportation. The views expressed in this paper are those of the authors and not necessarily those of COMET. The authors express their appreciation to Dr. J. H. Van Gerpen, Department of Mechanical Engineering at Iowa State University, for information on IC engine performance and to Reatha Diedrichs for help in preparation of the manuscript.

APPENDIX A

Thermal Analysis of the Exhaust System

Consider a system for thermal analysis of the exhaust system that is infinitesimal in extent along the flow axis. The combustion products with mass flow rate $\dot{m}_{ex}$ and constant pressure specific heat c_{pex} undergo a change in temperature of $dT_{ex}(x)$ as they move from axial location x to $x + dx$ (inside the exhaust pipe). An energy balance for this system yields

$$\frac{dT_{ex}}{dx} = -\frac{Ph_i h_{out}(T_{ex} - T_a)}{\dot{m}_{ex} c_{pex}(h_i + h_{out})}, \tag{A1}$$

where h_i is the convection heat transfer coefficient on the inside of the pipe system and is computed using the Nusselt number correlation:

$$\mathrm{Nu}_i = (f_r/8)\mathrm{Re}_{ex}\mathrm{Pr}_{ex}^{1/3}, \tag{A2}$$

where $\mathrm{Nu}_i = h_i D/k_{ex}$, D is the *equivalent diameter* for the exhaust system pipe, $P \sim \pi D$ is the pipe perimeter, and k_{ex} is the thermal conductivity of the exhaust gases; $\mathrm{Re}_{ex} = 4\dot{m}_{ex}/(\pi\mu_{ex}D)$ is the Reynolds number of the pipe flow, and μ_{ex} is the viscosity of the exhaust gases; and Pr_{ex} is the Prandtl number, and f_r is the friction factor inside the pipe (note that k_{ex}, μ_{ex}, and Pr_{ex} are functions of T_{ex}). The *equivalent convection coefficient* h_{out} on the outside of the pipe has contributions from radiation and convection. Because these modes operate in parallel, we may write $h_{out} = h_r + h_o$, where h_o is due to convection (see Table 5) and $h_r = \varepsilon\sigma(T_{ex} + T_a)(T_{ex}^2 + T_a^2)$ is due to radiation. By assuming an average value for the radiation coefficient h_r, Eq. (A1) is made linear and has the solution

$$\frac{(T_{ex} - T_a)}{(T_{exi} - T_a)} = \exp\left(-\frac{x}{x_{ex}}\right), \tag{A3}$$

where $T_{exi} \sim 980$ K is the inlet exhaust gas temperature (e.g., at the point where the exhaust gases leave the engine block and enter the exhaust manifold) and $x_{ex} = \dot{m}_{ex}c_{pex}(h_i + h_{out})/(Ph_i h_{out})$ is a characteristic pipe length scale. For the ULS traffic scenario, values of $f_r \sim 0.05$ (a very rough inside pipe surface), $D \sim 0.05$ m, *equivalent pipe length* $x_L \sim 8$ m (the exhaust system equivalent surface area is $A_p = \pi D x_L = 1.26$ m^2), $\mathrm{Re}_{ex} = 17\,000$; $h_i = 43$ W m^{-2} K^{-1}, and $h_o = 50$ W m^{-2} K^{-1} yield $h_r = 18$ W m^{-2} K^{-1} for an average exhaust gas temperature of 285°C, an average pipe wall temperature of $T_{pw} \approx 150$°C, an exhaust gas exit temperature of $T_{exe} \approx 77$°C, and an overall heat loss for the exhaust gases of 13.0 kW. Radiation accounts for 25% of this overall loss. For the case of stopped traffic, the outer convection coefficient is greatly reduced and radiation accounts for about 80% of the heat loss from the exhaust system.

The pipe length x_L used in the model is an equivalent length for the entire exhaust system, which contains numerous bends and changes in duct area. To first order, its value is set by the vehicle length; but this value was modified iteratively so that the model predictions for exit plane temperature T_{exe} matched actual measurements better at several engine power-generation levels.

APPENDIX B

Chemical Analysis of the Combustion Reaction

The stochiometric equation for complete combustion of liquid octane with theoretical air (treated as a mixture of oxygen and nitrogen only) is

$$\mathrm{C_8H_{18}} + 12.5(\mathrm{O_2} + 3.76\mathrm{N_2}) \rightarrow 8\mathrm{CO_2} + 9\mathrm{H_2O} + 47\mathrm{N_2}. \tag{B1}$$

For every mole of octane burned, 64 moles of products result. Of special interest are the following results: for $\dot{m}_{fuel} = 1.0$ g s^{-1} of liquid octane burned, (i) a total mass flow rate for the reaction of 16.1 g s^{-1} results and (ii) a water vapor flow rate of 1.4 g s^{-1} occurs in the product stream.

REFERENCES

Bogren, J., T. Gustavsson, and S. Lindquist, 1992: A description of a local climatological model used to predict temperature variations along stretches of road. *Meteor. Mag.*, **121,** 157–165.

Brown, B. G., and A. H. Murphy, 1996: Improving forecasting performance by combining forecasts: The example of road surface temperature forecasts. *Meteor. Appl.*, **3,** 257–265.

Gustavsson, T., and J. Bogren, 1991: Infrared thermography in applied road climatological studies. *Int. J. Remote Sens.*, **19,** 1311–1328.

Heywood, J. B., 1988: *Internal Combustion Engine Fundamentals.* McGraw-Hill, 925 pp.

Knollhoff, D. S., 2001: Analysis and interpretation of roadway weather data for winter highway maintenance. M.S. thesis, Dept. of Geological and Atmospheric Science, Iowa State University, 74 pp. [Available from 3010 Agronomy, Ames, IA 50011.]

Munson, B. R., D. F. Young, and T. H. Okiishi, 1990: *Fundamentals of Fluid Mechanics.* John Wiley and Sons, 843 pp.

Paltridge, G. W., and C. M. R. Platt, 1976: *Radiative Processes in Meteorology and Climatology*. Elsevier, 318 pp.

Rayer, P. J., 1987: The Meteorological Office forecast and road surface temperature model. *Meteor. Mag.*, **116,** 180–191.

Sass, B. H., 1992: A numerical model for prediction of road temperature and ice. *J. Appl. Meteor.*, **31,** 1499–1506.

Schlichting, H., 1979: *Boundary-Layer Theory*. 3d ed. McGraw-Hill, 817 pp.

Shao, J., 1990: A winter road surface temperature prediction model with comparison to others. Ph.D. thesis, University of Birmingham, United Kingdom, 245 pp. [Available from Central Library, University of Birmingham, Birmingham B15 2TT, United Kingdom.]

Surgue, J. G., J. E. Thornes, and R. D. Osborne, 1983: Thermal mapping of road surface temperatures. *Phys. Technol.*, **13,** 212–213.

Swinbank, W. C., 1963: Long-wave radiation from clear skies. *Quart. J. Roy. Meteor. Soc.*, **89,** 339–348.

Takle, E. S., 1990: Bridge and roadway frost occurrence and prediction by use of an expert system. *J. Appl. Meteor.*, **29,** 727–734.

Tennekes, J., and J. L. Lumley, 1972: *A First Course in Turbulence*. The MIT Press, 300 pp.

White, F. M., 1991: *Viscous Fluid Flow*. 2d ed. McGraw-Hill, 614 pp.